J. Fluid Mech. (1990), *vol.* 219, *pp.* 291–311
Printed in Great Britain

Hypersonic viscous interaction with strong blowing

By A. F. MESSITER AND M. D. MATARRESE
Department of Aerospace Engineering, The University of Michigan, Ann Arbor, MI 48109-2140, USA

(Received 16 June 1989)

Solutions are obtained for hypersonic viscous interaction along a flat plate in the presence of strong boundary-layer blowing, with inverse-square-root injection velocity, for laminar flow over a cold wall and with a power-law viscosity–temperature relation. In the strong-interaction region, self-similarity is preserved if the blowing is such that the thicknesses of the inviscid shock layer, viscous shear layer, and inviscid blown layer all have the same order of magnitude. The weak-interaction region is also considered, and an approximate interpolation is used to join the solutions for the surface pressure. Certain difficulties in asymptotic matching are discussed, and the extension to flow past a thin wedge is shown.

1. Introduction

Drastic changes in the pressure variation along a boundary layer can occur in the presence of strong surface blowing, especially if the blowing velocity is large enough that the boundary layer is completely 'blown off' from the surface. In that event a region of nearly inviscid injected fluid is present between the thin viscous layer and the wall, with the pressure distribution determined through an interaction with the external flow. For subsonic or for incompressible laminar flow asymptotic solutions beyond blowoff were given by Kassoy (1971) and by Klemp & Acrivos (1972). For supersonic speeds Cole & Aroesty (1968) considered strong blowing in limiting cases such that the thickness of the blown-off shear layer could be neglected.

Among other studies, only a few were primarily concerned with obtaining asymptotic solutions for strong blowing. Kubota & Fernandez (1968) solved the boundary-layer equations for compressible laminar flow in the limit of large mass injection. Wallace & Kemp (1969) followed Cole & Aroesty (1968) in considering examples for which the shear-layer thickness can be neglected. Smith & Stewartson (1973*b*) treated a supersonic boundary layer with uniform blowing that starts at a point downstream of the leading edge, choosing the velocity to have an order of magnitude consistent with triple-deck scaling. A good summary of this and other earlier work was given by Smith & Stewartson (1973*a*).

At hypersonic speeds interaction effects are present even in the absence of blowing. If a flat plate is placed in a uniform hypersonic flow, the boundary-layer displacement effect causes the appearance of a shock wave. Far enough downstream the pressure change across the shock wave is small ('weak interaction') but in a region further forward the pressure ratio across the shock becomes large ('strong interaction'). At points still closer to the leading edge, all relevant distances are of the same order of magnitude, so that the boundary-layer approximation fails, and the distinction between boundary layer, inviscid shock layer, and shock wave disappears ('merged-layer regime'). These effects have been discussed in the books by Hayes & Probstein

(1959) and by Stewartson (1964); additional details concerning asymptotic matching of the strong-interaction solutions have been given by Bush (1966) and by Lee & Cheng (1969).

Self-similarity for hypersonic strong interaction is preserved for surface blowing of a power-law form consistent with the usual interaction solutions. Li & Gross (1961) gave numerical results for the strong-interaction problem with weak blowing such that the boundary layer is not yet blown off. Of interest in the present work is the case of larger blowing velocity such that the injected gas occupies a 'blown layer' having thickness of the same order as the thickness of the viscous shear layer and the inviscid 'shock layer' between the viscous layer and the shock wave. The shock layer is described by hypersonic small-disturbance theory (Van Dyke 1954), the blown layer by 'inviscid boundary-layer equations' and the viscous layer by the usual boundary-layer equations, all in self-similar form. In the case considered here, the injected gas is taken to have density of the same order as the density in the undisturbed external flow, whereas the density in the high-temperature viscous layer is much lower. Solutions are described for each of the three layers, weak interaction further downstream is discussed for the same wall conditions, and the extension to wedge flow is shown.

2. Formulation

A semi-infinite flat plate is placed in a uniform hypersonic flow with velocity u_∞, pressure p_∞, density ρ_∞, temperature T_∞, Mach number M_∞, and viscosity coefficient μ_∞. Coordinates X and Y are measured along and normal to the plate, respectively, with origin at the leading edge. The non-dimensional velocity $\boldsymbol{u} = (u, v)$, pressure p, density ρ, temperature T, and viscosity coefficient μ are all referred to their undisturbed values. The viscosity is assumed to depend on the temperature through the power-law relation $\mu = T^\omega$, where $\frac{1}{2} < \omega < 1$; the case $\omega = 1$ is also considered briefly.

The non-dimensional continuity, momentum, and energy equations for steady flow can be written

$$\operatorname{div} \rho \boldsymbol{u} = 0, \tag{2.1}$$

$$\rho \boldsymbol{u} \cdot \boldsymbol{\nabla} \boldsymbol{u} + (\gamma M_\infty^2)^{-1} \boldsymbol{\nabla} p = Re^{-1} \operatorname{div} \boldsymbol{\tau}, \tag{2.2}$$

$$\rho \boldsymbol{u} \cdot \boldsymbol{\nabla}(\tfrac{1}{2}H) = Re^{-1} \operatorname{div} (\boldsymbol{\tau u} - \boldsymbol{q}), \tag{2.3}$$

where $\gamma = c_p/c_v$ is the ratio of specific heats; H is the total enthalpy, non-dimensionalized with $\frac{1}{2}u_\infty^2$; the coordinates are $x = X/X_r$ and $y = Y/X_r$, with X_r a reference length still to be defined; and $Re = u_\infty X_r/\nu_\infty$ is the Reynolds number, with $\nu_\infty = \mu_\infty/\rho_\infty$. The stress tensor is $\boldsymbol{\tau} = 2\mu\boldsymbol{\varepsilon} + \lambda \boldsymbol{I} \operatorname{div} \boldsymbol{u}$, where λ is the second viscosity coefficient, non-dimensionalized with μ_∞; $\boldsymbol{\varepsilon}$ is the rate-of-strain tensor; and $\boldsymbol{I}$ is the identity tensor. The heat conduction vector is $\boldsymbol{q} = -\mu \boldsymbol{\nabla} T/\{(\gamma-1)M_\infty^2 Pr\}$, where Pr is the Prandtl number. For simplicity the specific heats are taken to be constant; the injected gas is considered to be air; a perfect gas is assumed, so that $p = \rho T$; and the Prandtl number is taken equal to one.

The reference length X_r is chosen such that for $X \gg X_r$ the boundary layer has only a small effect on the external flow ('weak interaction') whereas for $X \ll X_r$ the changes in pressure are large in comparison with the undisturbed pressure ('strong interaction'); that is, the shock wave is very weak for $X \gg X_r$ but very strong for $X \ll X_r$. For weak interaction the shock wave has slope $\approx 1/M_\infty$, whereas the

streamline inclination resulting from the boundary-layer displacement effect is $O\{(M_\infty^{1+\omega}/Re^{\frac{1}{2}})(X_r/X)^{\frac{1}{2}}\}$. Requiring the latter expression to be much smaller than $1/M_\infty$ when $X \gg X_r$ leads to the choice $X_r = M_\infty^{4+2\omega}\nu_\infty/u_\infty$, and so the two large parameters M_∞ and Re are related by $Re = M_\infty^{4+2\omega}$. The coordinates then are defined by

$$x = X/X_r, \quad y = Y/X_r, \quad X_r = M_\infty^{4+2\omega}\nu_\infty/u_\infty. \tag{2.4}$$

The usual hypersonic viscous interaction parameter χ, based on a distance X, is proportional to $x^{-\frac{1}{2}}$. Solutions for the strong- and weak-interaction regimes are found by considering limits of (2.1)–(2.3) as $M_\infty \to \infty$ and $x \to 0$ or $x \to \infty$ respectively.

It is convenient to think first in terms of the dividing case, represented by equations obtained in the limit as $M_\infty \to \infty$ with x fixed. In this case the Mach number based on velocity normal to the shock wave is neither close to one nor large. With strong blowing the boundary layer is blown off the wall as a viscous free-shear layer, again described in the limit by the boundary-layer equations. An inviscid shock layer between the shock wave and the shear layer is described in a first approximation by the hypersonic-small-disturbance equations. The injected gas in a low-speed region below the shear layer is also described asymptotically by inviscid-flow equations. Solutions in adjacent regions are to be joined by appropriate asymptotic matching.

The non-dimensional stream function ψ (referred to $\rho_\infty u_\infty X_r$) is defined by

$$\psi_y = \rho u, \quad \psi_x = -\rho v. \tag{2.5}$$

It can be seen that the mass flow ψ will have different orders of magnitude in different parts of the flow. For $x = O(1)$, the shock wave is located at $y = O(1/M_\infty)$ and has slope $O(1/M_\infty)$; the mass flow crossing the shock wave is $\psi = O(1/M_\infty)$; and in the inviscid flow behind the shock wave $p-1 = O(1)$, $\rho = O(1)$, and $T = O(1)$. The viscous shear layer has high temperature $T = O(M_\infty^2)$, because some of the kinetic energy is converted to thermal energy, and low density $\rho = O(1/M_\infty^2)$, because $p = \rho T$. If diffusion and convection terms are required to be of the same order for $X = O(X_r)$, where X_r is defined by (2.4), the shear-layer thickness is $O(1/M_\infty)$, and since $u = O(1)$ the mass flow in the shear layer is $\psi = O(1/M_\infty^3)$. In the blown layer adjacent to the wall, the density ρ is $O(1)$ for the case to be considered, and for $p-1 = O(1)$ the momentum equation then gives $u = O(1/M_\infty)$. If the blown-layer thickness is also to be $O(1/M_\infty)$, the mass flow must be $\psi = O(1/M_\infty^2)$. The reference streamline is chosen such that $\psi > 0$ for air from the free stream and $\psi < 0$ for the blown gas; the streamline $\psi = 0$ lies within the shear layer.

It appears helpful to introduce notation which takes into account the different orders of magnitude in the different flow regions. For this purpose a hat, bar and tilde will denote variables in the inviscid shock layer, the viscous shear layer, and the inviscid blown layer, respectively. The corresponding stream-function coordinates are, respectively,

$$\hat{\psi} = M_\infty \psi, \quad \bar{\psi} = M_\infty^3 \psi, \quad \tilde{\psi} = M_\infty^2 \psi. \tag{2.6}$$

In the shock layer, the dependent variables are expanded in the form

$$v = M_\infty^{-1}\hat{v}(x, \hat{\psi}) + \ldots, \tag{2.7}$$

$$p = \hat{p}(x, \hat{\psi}) + \ldots, \tag{2.8}$$

$$\rho = \hat{\rho}(x, \hat{\psi}) + \ldots, \tag{2.9}$$

$$y = M_\infty^{-1}\hat{y}(x, \hat{\psi}) + \ldots, \tag{2.10}$$

for $0 < \hat{\psi} < \hat{\psi}_s$, where $\hat{\psi}_s$ is the value of $\hat{\psi}$ at the shock wave; also $u = 1 + \ldots$, and $\hat{T} = \hat{p}/\hat{\rho}$. In the shear layer,

$$u = \bar{u}(x, \bar{\psi}) + \ldots, \tag{2.11}$$

$$\rho = M_\infty^{-2}\,\bar{\rho}(x, \bar{\psi}) + \ldots, \tag{2.12}$$

$$T = M_\infty^2\,\bar{T}(x, \bar{\psi}) + \ldots, \tag{2.13}$$

$$y = M_\infty^{-1}\,\bar{y}(x, \bar{\psi}) + \ldots, \tag{2.14}$$

and $\bar{p} = \bar{\rho}\bar{T}$. The range for $\bar{\psi}$ is $\bar{\psi}_0(x) < \bar{\psi} < \infty$, where $\bar{\psi}_0(x) < 0$ is to be determined. In the blown layer,

$$u = M_\infty^{-1}\,\tilde{u}(x, \tilde{\psi}) + \ldots, \tag{2.15}$$

$$v = M_\infty^{-2}\,\tilde{v}(x, \tilde{\psi}) + \ldots, \tag{2.16}$$

$$\rho = \tilde{\rho}(x, \tilde{\psi}) + \ldots, \tag{2.17}$$

$$T = \tilde{T}(x, \tilde{\psi}) + \ldots, \tag{2.18}$$

$$y = M_\infty^{-1}\,\tilde{y}(x, \tilde{\psi}) + \ldots, \tag{2.19}$$

and $\tilde{p} = \tilde{\rho}\tilde{T}$. The range for $\tilde{\psi}$ is $\tilde{\psi}_w(x) < \tilde{\psi} < 0$, where $\tilde{\psi}_w(x)$ is the value of $\tilde{\psi}$ at the wall and is specified. The combined displacement effect of the viscous layer and blown layer implies an effective thin body shape

$$y = M_\infty^{-1}\,\Delta(x), \quad \Delta(x) = \bar{\Delta}(x) + \tilde{\Delta}(x), \tag{2.20}$$

where the functions $\bar{\Delta}(x)$ and $\tilde{\Delta}(x)$ represent, respectively, the contributions of the viscous and blown layers, to be determined. When M_∞ is large, omitted terms are small in comparison with terms retained in each of the expansions (2.7)–(2.19). Formulations for the strong- and weak-interaction problems are obtained by further expansion of (2.7)–(2.20) as $x \to 0$ or $x \to \infty$ respectively.

In the strong-interaction limit $x \to 0$, the hypersonic-small-disturbance equations possess a family of self-similar solutions corresponding to flows past thin power-law bodies. The viscous-layer equations likewise possess a family of self-similar solutions. If the solutions in the two regions are required to match correctly, it is found that the similarity variable (for y) must be $M_\infty\, y/x^{\frac{3}{4}}$ and the pressure in the viscous layer is $\bar{p} \sim \bar{p}_1\, x^{-\frac{1}{2}}$ (e.g. Stewartson 1964). In the presence of surface blowing the self-similarity is preserved if the blowing velocity and wall temperature are such that thickness of the blown layer is also $O(M_\infty^{-1}\, x^{\frac{3}{4}})$. The effective body shape $\Delta(x)$ then has the form

$$\Delta(x) \sim \Delta_1\, x^{\frac{3}{4}}, \quad \Delta_1 = \bar{\Delta}_1 + \tilde{\Delta}_1, \tag{2.21}$$

where $\bar{\Delta}_1$ and $\tilde{\Delta}_1$ are constants to be determined, and the contributions of the viscous and blown layers are $\bar{\Delta}(x) \sim \bar{\Delta}_1\, x^{\frac{3}{4}}$ and $\tilde{\Delta}(x) \sim \tilde{\Delta}_1\, x^{\frac{3}{4}}$. It also follows that the shock-wave slope $\mathrm{d}Y/\mathrm{d}X$ is no longer small when $x = O(M_\infty^{-4})$, i.e. when $X = O(M_\infty^{2\omega}\, \nu_\infty/u_\infty)$; a strong-interaction solution thus describes the flow region $M_\infty^{-4} \ll x \ll 1$. The various flow regions are indicated in figure 1.

For strong interaction it is seen, with the help of the shock-wave jump conditions, that the mass flow in the inviscid shock layer is $\psi = M_\infty^{-1}\,\hat{\psi} = O(M_\infty^{-1}\, x^{\frac{3}{4}})$. In the shear layer, the temperature is $T \sim M_\infty^2\,\bar{T} = O(M_\infty^2)$ and the density (from the perfect-gas law) is $\rho \sim M_\infty^{-2}\,\bar{\rho} = O(M_\infty^{-2}\, x^{-\frac{1}{2}})$; the velocity is $u = O(1)$, and so the mass flow is much smaller, namely $\psi = M_\infty^{-3}\,\bar{\psi} = O(M_\infty^{-3}\, x^{\frac{1}{4}})$. In the case to be considered here, the wall density is taken to be $\rho_w \sim \tilde{\rho}_w = O(1)$, and the Bernoulli equation for compressible flow gives $u \sim M_\infty^{-1}\,\tilde{u} = O(M_\infty^{-1}\, x^{-\frac{1}{4}})$ for the injected gas; the required mass flow $\psi = M_\infty^{-2}\,\tilde{\psi} = O(M_\infty^{-2}\, x^{\frac{1}{2}})$ in the blown layer is therefore provided by a blowing velocity $v_w \sim M_\infty^{-2}\,\tilde{v}_w = O(M_\infty^{-2}\, x^{-\frac{1}{2}})$. It follows, for example, that the mass flow $\rho_w\, v_w$ at the wall

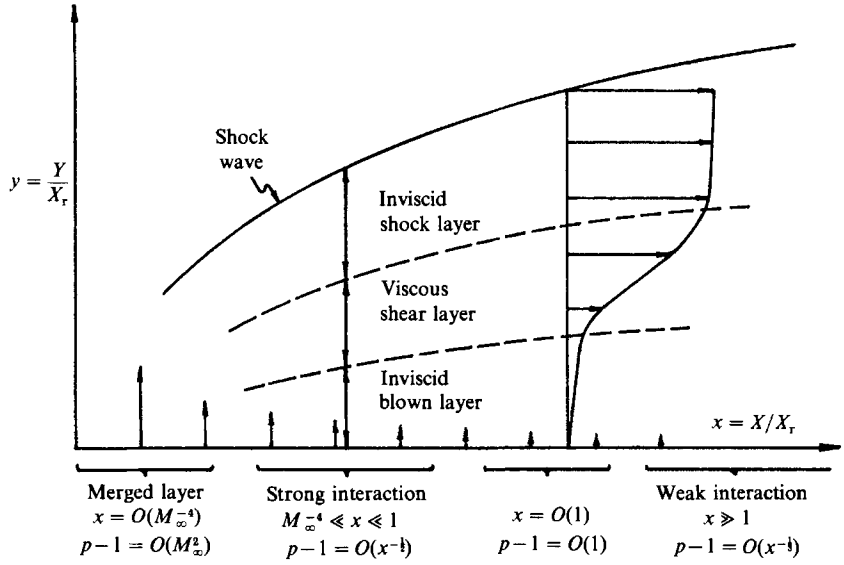

FIGURE 1. Flow regions for viscous interaction in hypersonic flow past a flat plate with strong blowing.

is smaller than the mass flow $\rho_\infty u_\infty \mathrm{d}(\Delta/M_\infty)/\mathrm{d}x$ through the shock wave by a factor $O(1/M_\infty)$, and that the wall shear stress $(\mu \partial u/\partial y)_w$ is smaller than the momentum flux $\rho_w v_w^2$ at the surface by a factor $O(M_\infty^{-2\omega})$. The three different mass flows suggest the three similarity variables (for ψ) needed for the inviscid shock layer, the viscous shear layer, and the inviscid blown layer:

$$\hat{\zeta} = \hat{\psi}/x^{\frac{3}{4}}, \quad \bar{\zeta} = \bar{\psi}/x^{\frac{1}{4}}, \quad \tilde{\zeta} = \tilde{\psi}/x^{\frac{1}{2}}. \tag{2.22}$$

The choices for the blown layer are, however, not unique. The required conditions (mass conservation, perfect-gas law, Bernoulli equation) are found to be satisfied if $M_w = (\text{const.}) M_\infty^{-1} x^{-\frac{1}{4}}$, where $M_w = M_\infty v_w T_w^{-\frac{1}{2}}$ is the Mach number of the injected gas at the surface. Another possible choice that would satisfy this requirement is $T_w =$ const. and $v_w = M_\infty^{-2} \tilde{v}_{1w} x^{-\frac{1}{4}}$, giving a mass flow $\tilde{\psi} = O(M_\infty^{-2} x^{\frac{1}{4}})$ that has the same x-dependence as the mass flow in the shear layer. This case corresponds more closely to the flows considered by Kubota & Fernandez (1968) and Li & Gross (1961). Although the wall temperature then would not match directly with the higher temperature in the merged-layer regime, the solution methods are otherwise the same, with some different details for the blown layer and for the final result relating surface pressure and blowing velocity.

The layer thicknesses and mass flows for strong interaction corresponding to (2.21) and (2.22) are summarized in figure 2. Solutions for the three regions can be obtained separately, each leading to a relation between pressure and a layer thickness, as shown in §3. First-order matching conditions then allow the results to be combined so as to determine the relation between surface pressure and blowing velocity. Some numerical results are described in §4.

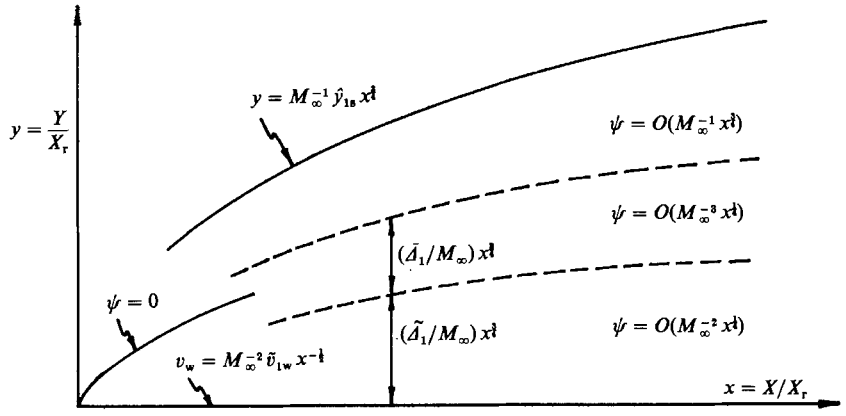

FIGURE 2. Orders of magnitude for layer thicknesses and mass flows in strong-interaction region.

3. Solutions

3.1. *Inviscid shock layer*

In a first approximation the inviscid flow at high Mach number past a thin two-dimensional body is equivalent to one-dimensional unsteady flow in a plane slab of fluid passing over the body at the undisturbed speed, and is described by the hypersonic small-disturbance equations (Van Dyke 1954). In terms of independent variables x and $\hat{\psi}$ the continuity, momentum, entropy, and streamline equations become, respectively,

$$(1/\hat{\rho})_x - \hat{v}_{\hat{\psi}} + \ldots = 0, \tag{3.1}$$

$$\hat{v}_x + \gamma^{-1}\hat{p}_{\hat{\psi}} + \ldots = 0, \tag{3.2}$$

$$\hat{p}_x - (\gamma\hat{p}/\hat{\rho})\hat{\rho}_x + \ldots = 0, \tag{3.3}$$

$$\hat{y}_{\hat{\psi}} - (1/\hat{\rho}) + \ldots = 0. \tag{3.4}$$

If the shock wave $\hat{\psi} = \hat{\psi}_s(x)$ is very strong, so that $\hat{\psi}_s' \gg 1$, the corresponding jump conditions across the shock are

$$\hat{\rho}_s = (\gamma+1)/(\gamma-1) + \ldots, \tag{3.5}$$

$$\hat{p}_s = 2\gamma\hat{\psi}_s'^2/(\gamma+1) + \ldots, \tag{3.6}$$

$$\hat{v}_s = 2\hat{\psi}_s'/(\gamma+1) + \ldots, \tag{3.7}$$

$$\hat{y}_s = \hat{\psi}_s, \tag{3.8}$$

where $\hat{\rho}_s = \hat{\rho}(x, \hat{\psi}_s)$, etc. As $\hat{\psi} \to 0$, at the inner 'edge' of the shock layer, $\hat{y} \to \Delta(x)$ and $\hat{v} \to \Delta'(x)$.

In the limit as $M_\infty \to \infty$, $x \to 0$, and $\hat{\psi} \to 0$ such that $M_\infty^4 x \to \infty$ and $\hat{\zeta} = \hat{\psi}/x^{\frac{3}{4}}$ is held fixed, the functions appearing in (2.7)–(2.10) can be expressed in self-similar form by

$$\hat{v} = x^{-\frac{1}{4}}\hat{v}_1(\hat{\zeta}) + \ldots, \tag{3.9}$$

$$\hat{p} = x^{-\frac{1}{2}}\hat{p}_1(\hat{\zeta}) + \ldots, \tag{3.10}$$

$$\hat{\rho} = \hat{\rho}_1(\hat{\zeta}) + \ldots, \tag{3.11}$$

$$\hat{y} = x^{\frac{3}{4}}\hat{y}_1(\hat{\zeta}) + \ldots, \tag{3.12}$$

Substitution into (3.1)–(3.4) then provides a system of first-order nonlinear ordinary

differential equations, subject to boundary conditions found from the shock relations (3.5)–(3.8). The entropy equation can be integrated to give a relation between $\hat{p}_1$ and $\hat{\rho}_1$:

$$\hat{\rho}_1^{\gamma} = \left(\frac{\gamma+1}{\gamma-1}\right)^{\gamma} \frac{\gamma+1}{2\gamma} \left(\frac{4}{3}\right)^2 \left(\frac{\Delta_1}{\hat{y}_{1s}}\right)^2 \left(\frac{\hat{p}_1}{\Delta_1^2}\right) \left(\frac{\hat{\zeta}}{\hat{y}_{1s}}\right)^{\frac{2}{3}}. \tag{3.13}$$

Numerical integration of the remaining equations for $\gamma = 1.4$, with $\hat{y}_1 \to \Delta_1$ and $\hat{v}_1 \to \frac{3}{4}\Delta_1$ as $\hat{\zeta} \to 0$, leads to the values

$$\hat{p}_1(0)/\Delta_1^2 = 1.1194, \quad \Delta_1/\hat{y}_{1s} = 0.5912, \tag{3.14}$$

which agree with values given by Brown & Stewartson (1975) and by Li & Gross (1961). Since $\hat{p}_1 \sim$ constant as $\hat{\zeta} \to 0$, (3.13) shows that $\hat{\rho}_1 = O(\hat{\zeta}^{2/(3\gamma)})$ as $\hat{\zeta} \to 0$. Solutions for the viscous and blown layers are now needed to determine Δ_1 in terms of the blowing velocity at the surface.

3.2. *Inviscid blown layer*

Solutions for the blown layer follow directly from the results of Cole & Aroesty (1968). Since the layer is thin, in a first approximation the pressure is a function only of x and the differential equations are 'inviscid boundary-layer equations':

$$\tilde{\rho}\tilde{u}\tilde{u}_x + \gamma^{-1}\tilde{p}_x + \ldots = 0, \tag{3.15}$$

$$\tilde{p}_{\tilde{\psi}} + \ldots = 0, \tag{3.16}$$

$$\tilde{p}_x - (\gamma\tilde{p}/\tilde{\rho})\tilde{\rho}_x + \ldots = 0, \tag{3.17}$$

$$\tilde{y}_{\tilde{\psi}} - (\tilde{\rho}\tilde{u})^{-1} = 0, \tag{3.18}$$

where $\tilde{p} = \tilde{p}(x)$. The mass flow at the wall is $\tilde{\psi} = \tilde{\psi}_w(x)$, where $\mathrm{d}\tilde{\psi}_w = -\tilde{\rho}_w \tilde{v}_w \,\mathrm{d}x$; the inverse relationship $x = x_w(\tilde{\psi})$, where $\mathrm{d}x_w = -(\tilde{\rho}_w \tilde{v}_w)^{-1}\,\mathrm{d}\tilde{\psi}$, identifies a streamline by the location at which it leaves the wall. At the wall the density $\tilde{\rho}_w$ and the blowing velocity $\tilde{v}_w$ are to be specified, and can be expressed by evaluating $\tilde{\rho}$ and $\tilde{v}$ either at x and $\tilde{\psi}_w(x)$ or at x_w and $\tilde{\psi}(x_w)$. The latter interpretation is needed in most of the following, so $\tilde{\rho}_w$ and $\tilde{v}_w$ will denote quantities which are constant along streamlines. Integration of the entropy and momentum equations leads to solutions for $\tilde{\rho}$ and $\tilde{u}$ in terms of x and x_w:

$$\tilde{\rho} = \left(\frac{\tilde{p}}{\tilde{p}_w}\right)^{1/\gamma} \tilde{\rho}_w + \ldots, \tag{3.19}$$

$$\tilde{u}^2 = \frac{2}{\gamma-1}\tilde{T}_w \left\{1 - \left(\frac{\tilde{p}}{\tilde{p}_w}\right)^{(\gamma-1)/\gamma}\right\} + \ldots, \tag{3.20}$$

where $\tilde{p} = \tilde{p}(x)$ and $\tilde{p}_w = \tilde{p}(x_w)$; $\tilde{T}_w = \tilde{p}_w/\tilde{\rho}_w$ is the wall temperature, as a function of x_w.

If now $x \to 0$ with $\tilde{\zeta} = \tilde{\psi}/x^{\frac{1}{2}}$ fixed, where $\tilde{\zeta}_w < \tilde{\zeta} < 0$, the solutions can be expanded in the form

$$\tilde{u} = x^{-\frac{1}{4}}\tilde{u}_1(\tilde{\zeta}) + \ldots, \tag{3.21}$$

$$\tilde{v} = x^{-\frac{1}{2}}\tilde{v}_1(\tilde{\zeta}) + \ldots, \tag{3.22}$$

$$\tilde{\rho} = \tilde{\rho}_1(\tilde{\zeta}) + \ldots, \tag{3.23}$$

$$\tilde{p} = x^{-\frac{1}{2}}\tilde{p}_1 + \ldots, \tag{3.24}$$

$$\tilde{y} = x^{\frac{3}{4}}\tilde{y}_1(\tilde{\zeta}) + \ldots, \tag{3.25}$$

where $\tilde{p}_1$ is a constant to be determined, the blowing velocity is $\tilde{v}_w = x_w^{-\frac{1}{2}}\tilde{v}_{1w}$, and

$\tilde{\zeta}_w = -2\tilde{\rho}_{1w}\tilde{v}_{1w}$ is a specified constant. With $\tilde{p}_w \sim \tilde{p}_1 x_w^{-\frac{1}{2}}$ and $\xi = x_w/x$, the streamline shapes are found by substituting the expansions of (3.19) and (3.20) in (3.18):

$$d\tilde{y}_1 = -\left(\frac{\gamma-1}{2\tilde{T}_{1w}}\right)^{\frac{1}{2}} \tilde{v}_{1w}\, \xi^{-(\gamma+2)/(4\gamma)}(1-\xi^{(\gamma-1)/(2\gamma)})^{-\frac{1}{2}} d\xi, \tag{3.26}$$

where $\tilde{T}_1 = \tilde{p}_1/\tilde{\rho}_1$, $\tilde{T}_{1w} = \tilde{T}_1(\tilde{\zeta}_w)$, etc. The effective layer thickness $\tilde{\Delta}_1 x^{\frac{3}{4}}$ is found by integration between 0 and 1. After a change of variable $\eta = \xi^{(\gamma-1)/(2\gamma)}$,

$$\begin{aligned}\tilde{\Delta}_1 &= \left(\frac{2\tilde{\rho}_{1w}}{(\gamma-1)\tilde{p}_1}\right)^{\frac{1}{2}} \gamma\tilde{v}_{1w}\int_0^1 \eta^{(\gamma/2)/(\gamma-1)}(1-\eta)^{-\frac{1}{2}} d\eta \\ &= \{2\pi(\gamma-1)\}^{\frac{1}{2}}\frac{2\gamma^2}{2\gamma-1}\left(\frac{\tilde{\rho}_{1w}\tilde{v}_{1w}^2}{\tilde{p}_1}\right)^{\frac{1}{2}} \Gamma\left(\frac{\gamma}{2(\gamma-1)}\right)\Big/\Gamma\left(\frac{1}{2(\gamma-1)}\right),\end{aligned} \tag{3.27}$$

in agreement with a result of Cole & Aroesty (1968). For $\gamma = 1.4$,

$$\tilde{\Delta}_1 = 3.501(\tilde{r}_{1w}\tilde{v}_{1w}^2/\tilde{p}_1)^{\frac{1}{2}}.$$

If the shear-layer thickness were negligible, i.e. if $\bar{\Delta}_1 \ll \tilde{\Delta}_1$, then $\Delta_1 \approx \tilde{\Delta}_1$ and the surface pressure would be found by substituting this result in (3.14), with $\tilde{p}_1 = \hat{p}_1(0)$. In the case of primary interest here, however, $\bar{\Delta}_1$ cannot be neglected; the required shear-layer solution is given in the next subsection.

In the weak-interaction region downstream, for $x \gg 1$, the form of solution is different because pressure changes are small rather than large. If the blowing velocity remains $v_w(x) = M_\infty^{-2}\tilde{v}_{1w}x^{-\frac{1}{2}} = M_\infty^{\omega}\tilde{v}_{1w}(u_\infty X/\nu_\infty)^{-\frac{1}{2}}$ for $x \gg 1$, the mass flow in the blown layer is again $\tilde{\psi} = O(x^{\frac{1}{2}})$. The pressure perturbation $\tilde{p}-1$, in a first approximation, is now proportional to the slope $d\Delta/dx$ of the equivalent body. From the Bernoulli equation, the velocity $\tilde{u}$ is $O((\tilde{p}-1)^{\frac{1}{2}})$. A mass-flow balance for the blown layer then shows that, for $x \gg 1$,

$$\tilde{p}-1 = x^{-\frac{1}{6}}\tilde{\tilde{p}}_1+\ldots, \tag{3.28}$$

$$\tilde{u} = x^{-\frac{1}{6}}\tilde{\tilde{u}}_1(\tilde{\zeta})+\ldots, \tag{3.29}$$

$$\tilde{y} = x^{\frac{2}{3}}\tilde{\tilde{y}}_1(\tilde{\zeta})+\ldots, \tag{3.30}$$

where a double tilde is used to distinguish where necessary from the symbols introduced for $x \ll 1$. The solutions are found in the same way as for $x \ll 1$, but are simpler in form because the density $\tilde{\rho} \sim \tilde{\rho}_{1w}$ is nearly constant for $x \gg 1$:

$$\tilde{\tilde{u}}_1^2 = \frac{2\tilde{\tilde{p}}_1}{\gamma\tilde{\rho}_{1w}}\left\{\left(\frac{2\tilde{\rho}_{1w}\tilde{v}_{1w}}{-\tilde{\psi}}\right)^{\frac{2}{3}} x^{\frac{1}{3}}-1\right\}, \tag{3.31}$$

$$\tilde{\tilde{p}}_1 = \tfrac{2}{3}\gamma\tilde{\tilde{\Delta}}_1 = 2(\tfrac{2}{3})^{\frac{2}{3}}\gamma(\tilde{\rho}_{1w}\tilde{v}_{1w}^2)^{\frac{1}{3}}, \tag{3.32}$$

where the effective thickness is $\tilde{\tilde{\Delta}}(x) = \tilde{\tilde{\Delta}}_1 x^{\frac{2}{3}}$. The constant-pressure shear layer for $x \gg 1$ has only a higher-order effect since its thickness $\bar{\Delta}(x) = O(x^{\frac{1}{2}})$ is small in comparison with the blown-layer thickness $\tilde{\Delta}(x)$. The air that has passed through the strong shock wave further upstream, and therefore has higher entropy, contributes still another higher-order displacement effect that likewise can be neglected in a first approximation. The value (3.32) is consistent with the results of Cole & Aroesty (1968).

3.3. *Viscous shear layer*

The viscous shear layer is described in a first approximation as a mixing layer between air moving with uniform speed at zero temperature and another gas, here taken also to be air, at rest with zero temperature. In terms of independent variables x and $\bar{\psi}$ the boundary-layer approximations to the momentum, total-enthalpy, and streamline equations are

$$\bar{u}_x + \frac{\bar{T}}{\gamma \bar{p} \bar{u}} \bar{p}_x = \bar{p}(\bar{T}^{\omega-1} \bar{u} \bar{u}_{\bar{\psi}})_{\bar{\psi}} + \ldots, \tag{3.33}$$

$$\bar{H}_x = \bar{p}(\bar{T}^{\omega-1} \bar{u} \bar{H}_{\bar{\psi}})_{\bar{\psi}} + \ldots, \tag{3.34}$$

$$\bar{y}_{\bar{\psi}} = (\bar{\rho}\bar{u})^{-1}, \tag{3.35}$$

where $\bar{H} = \bar{u}^2 + 2\bar{T}/(\gamma - 1)$.

Asymptotic representations of the solutions as $x \to 0$ are expressed in terms of the similarity variable $\bar{\zeta} = \bar{\psi}/x^{\frac{1}{4}}$, for $\bar{\zeta}_0 < \bar{\zeta} < \infty$, in the form

$$\bar{u} = \bar{u}_1(\bar{\zeta}) + \ldots, \tag{3.36}$$

$$\bar{T} = \bar{T}_1(\bar{\zeta}) + \ldots, \tag{3.37}$$

$$\bar{p} = x^{-\frac{1}{2}} \bar{p}_1 + \ldots, \tag{3.38}$$

$$\bar{y} = x^{\frac{3}{4}} \bar{y}_1(\bar{\zeta}) + \ldots, \tag{3.39}$$

where $\bar{\zeta}_0 < 0$ and $\bar{p}_1 =$ constant; also $\bar{\rho} = \bar{p}/\bar{T}$. The value of $\bar{\zeta}_0$, which characterizes the amount of mass entrained in the lower part of the shear layer, is to be determined. Substitution gives the ordinary differential equations

$$-\tfrac{1}{4}\bar{\zeta}\bar{u}_1' - \frac{\bar{T}_1}{2\gamma \bar{u}_1} = \bar{p}_1(\bar{T}_1^{\omega-1} \bar{u}_1 \bar{u}_1')', \tag{3.40}$$

$$-\tfrac{1}{4}\bar{\zeta}\bar{T}_1' + \frac{\gamma - 1}{2\gamma} \bar{T}_1 = \bar{p}_1(\bar{T}_1^{\omega-1} \bar{u}_1 \bar{T}_1')' + (\gamma - 1)\, \bar{p}_1 \bar{T}_1^{\omega-1} \bar{u}_1 \bar{u}_1'^2, \tag{3.41}$$

$$\bar{y}_1' = \bar{T}_1/(\bar{p}_1 \bar{u}_1). \tag{3.42}$$

The solutions should match with the shock-layer solutions as $\bar{\zeta} \to \infty$ and with the blown-layer solutions as $\bar{\zeta} \to \bar{\zeta}_0$. Thus it is required that $\bar{u}_1 \to 1$, $\bar{T}_1 \to 0$ as $\bar{\zeta} \to \infty$ and $\bar{u}_1 \to 0$, $\bar{T}_1 \to 0$ as $\bar{\zeta} \to \bar{\zeta}_0$. The effective layer thickness is $\Delta_1 x^{\frac{3}{4}}$, where Δ_1 is the integral of (3.42) from $\bar{\zeta}_0$ to ∞; the integral is finite because the temperature decreases sufficiently rapidly as $\bar{\zeta} \to \bar{\zeta}_0$. The numerical solution is carried out in terms of a rescaled independent variable $\bar{p}_1^{-\frac{1}{4}} \bar{\zeta}$, and $\bar{p}_1$ is to be found later from the appropriate matching conditions.

The differential equations (3.40) and (3.41) are singular at $\bar{\zeta} = \bar{\zeta}_0$. For $\frac{1}{2} < \omega < 1$, the range of particular interest, the solutions as $\bar{\zeta} \to \bar{\zeta}_0$ have the form $\bar{u}_1 = (\bar{\zeta} - \bar{\zeta}_0)^{\alpha} u^{\dagger}$ and $\bar{T}_1 = (\bar{\zeta} - \bar{\zeta}_0)^{\beta} T^{\dagger}$, where $u^{\dagger}$ and $T^{\dagger}$ are analytic, and the exponents are $\alpha = \omega/(2\omega - 1)$ and $\beta = 1/(2\omega - 1)$. The coefficients $\bar{T}_1^{\omega-1} \bar{u}_1$ of the second derivatives in (3.40) and (3.41) are therefore $O(\bar{\zeta} - \bar{\zeta}_0)$ as $\bar{\zeta} \to \bar{\zeta}_0$. The numerical integration, described in detail elsewhere (Matarrese & Messiter 1990), is based on a Newton iteration scheme, starting from simple assumed distributions for $\bar{u}_1$ and $\bar{T}_1$ over a range $\bar{\zeta}_L < \bar{\zeta} < \infty$. Initially the lower limit $\bar{\zeta}_L$ is chosen large enough to ensure that $\bar{\zeta}_L > \bar{\zeta}_0$. However, the solutions thus obtained for $\bar{u}_1$ and $\bar{T}_1$ do not have the correct asymptotic behaviour when $\bar{\zeta} \to \bar{\zeta}_L$. Next $\bar{\zeta}_L$ is decreased until the numerical and asymptotic solutions are seen to agree closely for small $\bar{u}_1$ and $\bar{T}_1$; the value found for

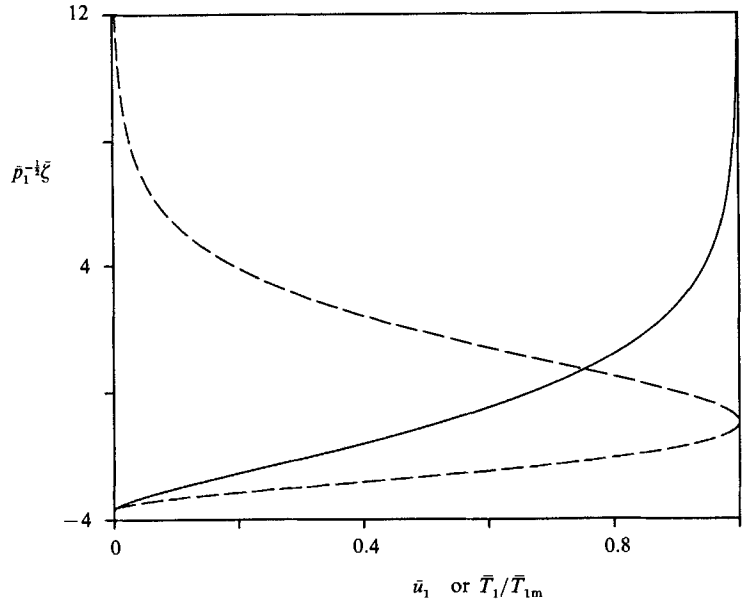

FIGURE 3. Scaled shear-layer solutions in strong-interaction limit, as functions of the stream-function variable $\bar{p}_1^{-\frac{1}{2}}\bar{\zeta} = \bar{p}_1^{-\frac{1}{2}}M_\infty^3\bar{\psi}/x^{\frac{1}{2}}$, for $\omega = 0.75$: ——, velocity $\bar{u}_1$; – – –, temperature $\bar{T}_1/\bar{T}_{1m}$.

$\bar{p}^{-\frac{1}{2}}\bar{\zeta}_0$ is believed to be accurate to within less than 0.1 %. The results for $\gamma = 1.4$ and $\omega = 0.75$ are

$$\bar{p}_1^{-\frac{1}{2}}\bar{\zeta}_0 = -3.683, \quad \bar{p}_1^{-\frac{1}{2}}\bar{\Delta}_1 = 0.3518. \tag{3.43}$$

The corresponding velocity and temperature functions $\bar{u}_1$ and $\bar{T}_1$ are plotted against $\bar{p}_1^{-\frac{1}{2}}\bar{\zeta}$ in figure 3, for $\bar{p}_1^{-\frac{1}{2}}\bar{\zeta}_0 < \bar{p}_1^{-\frac{1}{2}}\bar{\zeta} < \infty$; $\bar{T}_1$ has been normalized with its maximum value $\bar{T}_{1m}$.

Calculation of the pressure is completed by matching $\bar{p}_1$ as $\bar{\zeta} \to \infty$ with the shock-layer pressure $\hat{p}_1$ evaluated as $\hat{\zeta} \to 0$ and matching $\bar{p}_1$ as $\bar{\zeta} \to \bar{\zeta}_0$ with the blown-layer pressure $\tilde{p}_1$ as $\tilde{\zeta} \to 0$. Thus

$$\tilde{p}_1 = \bar{p}_1 = \hat{p}_1(0). \tag{3.44}$$

Now (3.14), (3.27), and (3.43) can be combined to eliminate the layer thicknesses, as shown in §4 below.

If $\omega \to \frac{1}{2}$, the exponents α and β obtained above in the solutions for $\bar{\zeta} \to \bar{\zeta}_0$ will both become infinite, and clearly a different kind of asymptotic form is required. Numerical solutions for $\omega = 0.7$ and $\omega = 0.6$, not shown here, suggest that the lower limit $\bar{\zeta}_0 \to -\infty$ as $\omega \to \frac{1}{2}$. When $\omega = \frac{1}{2}$, it then follows from (3.40) and (3.41) that $\bar{u}_1$ and $\bar{T}_1$ become exponentially small as $\bar{\zeta} \to -\infty$.

For $\omega = 1$ the asymptotic behaviour as $\bar{\zeta} \to \bar{\zeta}_0$ seems easier to understand in terms of Howarth variables defined by $\mathrm{d}Y = \bar{\rho}\,\mathrm{d}\bar{y}$, $\mathrm{d}X = \bar{p}\,\mathrm{d}x$ and the similarity variable $\eta = Y/(2X)^{\frac{1}{2}}$. The stream function and total enthalpy are $\bar{\psi} = (2X)^{\frac{1}{2}}F(\eta) + \ldots$ and $H = G(\eta) + \ldots$ respectively, where F and G satisfy the ordinary differential equations $F''' + FF'' = \gamma^{-1}(\gamma - 1)(F'^2 - G)$ and $G'' + FG' = 0$. As $\eta \to -\infty$, $G = O(\mathrm{e}^\eta)$ and $F - F_0 = O(\eta\,\mathrm{e}^\eta)$, with F_0 (corresponding to $\bar{\zeta}_0$) to be determined; the fact that

$$G = O\{(F - F_0)/\ln(F - F_0)\}$$

as $\eta \to -\infty$ implies the presence of a logarithm in $\bar{T}_1$ as $\bar{\zeta} \to \bar{\zeta}_0$. The numerical solution when $\omega = 1$ can be obtained by a shooting method to give

$$\bar{p}_1^{-\frac{1}{2}} \bar{\zeta}_0 = -2.066, \quad \bar{p}_1^{-\frac{1}{2}} \bar{A}_1 = 0.2100. \tag{3.45}$$

3.4. *Higher-order matching*

Matching of the shock-layer and shear-layer solutions requires for each variable that the solutions evaluated as $\hat{\zeta} \to 0$ and $\bar{\zeta} \to \infty$ agree term by term. As $\hat{\zeta} \to 0$, the inner edge of the shock layer is approached from above and the hypersonic-small-disturbance solutions (3.13) and (3.14) show that the temperature has the form $T \sim \hat{T} = \hat{p}/\hat{\rho} = x^{-\frac{1}{2}} \hat{p}_1/\hat{\rho}_1 + \ldots = O(x^{-\frac{1}{2}} \hat{\zeta}^{-2/(3\gamma)})$ as $x \to 0$ and $\hat{\zeta} \to 0$. However, as $\bar{\zeta} \to \infty$, the outer edge of the shear layer is approached from below and it follows from (3.41) that $T \sim M_\infty^2 \bar{T} = M_\infty^2 \bar{p}/\bar{\rho} = O(\bar{\zeta}^{-2/(1-\omega)})$. Since these two representations for T are not the same, the matching is not complete. Bush (1966) has shown that an additional 'layer' is required between the shock layer and the shear layer. A solution for T in terms of a variable $\zeta_B = M_\infty^A \psi/x^C$, for proper choices of the exponents A and C, allows matching in a first approximation with $\hat{T}$ as $\zeta_B \to \infty$ and with $M_\infty^2 \bar{T}$ as $\zeta_B \to 0$. When $\omega = 1$, the solution for $\bar{T}$ decays exponentially as $\bar{\zeta} \to \infty$; Lee & Cheng (1969) have shown that the matching difficulty is resolved not by adding another layer but by including higher-order terms in the shock-layer and shear-layer solutions.

Another difficulty arises with respect to matching of the shear-layer and blown-layer solutions. As $\bar{\zeta} \to \bar{\zeta}_0$, the inner edge of the shear layer is approached from above with $u \sim \bar{u} = O\{(\bar{\zeta} - \bar{\zeta}_0)^{\omega/(2\omega-1)}\}$ and $T \sim M_\infty^2 \bar{T} = O\{M_\infty^2 (\bar{\zeta} - \bar{\zeta}_0)^{1/(2\omega-1)}\}$. As $\tilde{\zeta} \to 0$, the outer edge of the blown layer is approached from below with $u \sim M_\infty^{-1} \tilde{u} = O\{M_\infty^{-1} x^{-\frac{1}{4}} (-\tilde{\zeta})^{-\frac{1}{2}}\}$ and $T \sim \tilde{T} = \tilde{p}/\tilde{\rho} = O\{x^{-\frac{1}{2}} (-\tilde{\zeta})^{-1/\gamma}\}$. The matching again is not complete, and it is not entirely clear how to proceed. For a first attempt, one might think that an additional solution is needed in a region between the shear layer and the blown layer, for $\bar{\psi}$ close to $x^{\frac{1}{4}} \bar{\zeta}_0$ and $\tilde{\psi}$ close to $M_\infty^{-1} x^{\frac{1}{4}} \bar{\zeta}_0$. The blown-layer and viscous-layer solutions for u would then be required to match with this new solution. If the matching for u is considered first, one is led to introduce a similarity variable

$$\zeta^* = (M_\infty x^{\frac{1}{4}})^{-1/(2\omega)} M_\infty (\bar{\psi} - x^{\frac{1}{4}} \bar{\zeta}_0), \tag{3.46}$$

and to try representations

$$\bar{u} = (M_\infty x^{\frac{1}{4}})^{-\frac{1}{2}} u_1^*(\zeta^*) + \ldots, \tag{3.47}$$

$$\bar{T} = (M_\infty x^{\frac{1}{4}})^{-1/(2\omega)} T_1^*(\zeta^*) + \ldots, \tag{3.48}$$

for $-\infty < \zeta^* < \infty$. However, this procedure leads to approximate equations that are just simplified versions of (3.40) and (3.41), with $\bar{\zeta} \approx \bar{\zeta}_0$ and $\bar{u}_1^2 \ll \bar{T}_1$. Except for additive integration constants, the solutions are already contained within the solutions to (3.40) and (3.41) and are not sufficient to allow the proper functional forms for both $\zeta^* \to -\infty$ and $\zeta^* \to \infty$. It is probably necessary both to include higher-order terms and to consider still other limit processes for a complete description of the local asymptotic structure. These details are not needed if only a first approximation to the pressure is desired.

If instead $\omega = 1$ the definition (3.46) for ζ^* again is appropriate, as is the representation (3.47) for u, but T has the modified form

$$\bar{T} = \{(M_\infty x^{\frac{1}{4}})^{\frac{1}{2}} \ln (M_\infty x^{\frac{1}{4}})\}^{-1} T_1^*(\zeta^*) + \ldots. \tag{3.49}$$

The presence of the logarithm is associated with the exponential forms of u and T in terms of the Howarth variables noted at the end of the preceding subsection. As a

result, the pressure-gradient term is absent from the momentum equation and two integrations can be carried out directly to give

$$(u_1^* - u_{10}^*) + u_{10}^* \ln (u_1^* - u_{10}^*) = -\bar{\zeta}_0 \zeta^*/(4\bar{p}_1), \tag{3.50}$$

where $u_{10}^* = 2(\bar{p}_1 \tilde{v}_{1w})^{\frac{1}{2}}/\{(\gamma-1)(-\bar{\zeta}_0)\}^{\frac{1}{2}}$, for matching with (3.20). It follows also that

$$T_1^* = (\text{const.})(u_1^* - u_{10}^*). \tag{3.51}$$

The representations for u and T match properly as $\zeta^* \to \infty$, and u approaches a small constant value as $\zeta^* \to -\infty$, but T_1^* is exponentially small as $\zeta^* \to -\infty$ and higher-order terms would be needed for completeness, as at the outer edge of the shear layer (Lee & Cheng 1969).

These considerations indicate some of the difficulties encountered in attempting to derive higher-order terms and thus to obtain estimates of the largest neglected effects. For $x = O(1)$, it is fairly easy to see that the relative errors in the differential equations obtained in each of the three limits (shock layer, viscous layer, blown layer) are all $O(M_\infty^{-2})$. The expansions of the flow variables as $M_\infty \to \infty$ would then seem to proceed in integer powers of M_∞^2. But the higher-order terms not yet matched will evidently require larger correction terms, probably in all three flow regions. It is therefore not possible to assess the error without further consideration of the next terms in each of the expansions. Moreover, in the strong-interaction limit $x \to 0$ the solutions will have expansions in positive powers of $x^{\frac{1}{4}}$ and $(M_\infty x^{\frac{1}{4}})^{-1}$, and in the weak-interaction limit $x \to \infty$ the solutions will be found as series expansions in negative powers of x, so that still other higher-order terms would have to be considered.

An additional question concerns the behaviour of the flow for weaker blowing. If the blowing velocity is decreased by taking $\tilde{v}_{1w} \ll 1$, the injected mass $|\psi| = 2M_\infty^{-2} \tilde{\rho}_{1w} \tilde{v}_{1w} x^{\frac{1}{2}}$ remains large in comparison with the mass flow $M_\infty^{-3} x^{\frac{1}{4}} |\zeta_0|$ in the lower part of the shear layer for values of x such that $M_\infty x^{\frac{1}{4}} \gg \tilde{v}_{1w}^{-1}$. The location of blowoff is at $x = O(M_\infty \tilde{v}_{1w})^{-4}$ and moves downstream as $\tilde{v}_{1w}$ decreases from $O(1)$ to $O(M_\infty^{-1})$. When $\tilde{v}_{1w} = O(M_\infty^{-1})$, the boundary layer is attached throughout the strong-interaction region $x \ll 1$, and in the weak-interaction region $x \gg 1$ the injected mass is of the same order as the mass flow $O(M_\infty^{-3} x^{\frac{1}{2}})$ required for the constant-pressure free shear layer. A special solution is needed for a narrow range of $M_\infty \tilde{v}_{1w}$ close to a dividing value, as for incompressible flow (Kassoy 1971; Klemp & Acrivos 1972).

3.5. *Wedge flow*

Inviscid hypersonic flow past a thin wedge is easily described with the help of suitable approximations to the shock-wave jump conditions. If the wedge half-angle is $\alpha \ll 1$, and $M_\infty \alpha \gg 1$, (3.5) gives $\rho \sim (\gamma+1)/(\gamma-1)$, and (3.6) with the shock slope $M_\infty \hat{y}_s' \sim \frac{1}{2}(\gamma+1) M_\infty \alpha$ gives $p \sim \frac{1}{2}\gamma(\gamma+1) M_\infty^2 \alpha^2$ in the uniform flow between the shock wave and the wedge surface; the Mach number there is $M \sim \{\frac{1}{2}\gamma(\gamma-1)\}^{-\frac{1}{2}} \alpha^{-1}$. If now a boundary layer is considered, its temperature is again $T = O(M_\infty^2)$, but the density $\rho = p/T$ is $O(\alpha^2)$. For weak interaction the boundary-layer thickness is

$$O\{M_\infty^\omega \alpha^{-1} (\nu_\infty X/u_\infty)^{\frac{1}{2}}\},$$

smaller by a factor $O(M_\infty^{-1} \alpha^{-1})$ than for a flat plate. This thickness is small in comparison with the distance $\frac{1}{2}(\gamma-1)\alpha X$ between wedge surface and shock wave, and the shock wave is therefore weak, only if $X \gg M_\infty^{2\omega} \alpha^{-4} \nu_\infty/u_\infty$. The reference length X_r should therefore be $X_r = M_\infty^{2\omega} \alpha^{-4} \nu_\infty/u_\infty$ for the wedge, smaller by a factor $(M_\infty \alpha)^{-4}$ than for a flat plate. The non-dimensional coordinates x, y and ψ are now defined in

terms of this new X_r. The scaled y-coordinates, however, are measured relative to the surface, with M_∞^{-1} replaced by α, so that

$$\tilde{y} = \hat{y} = (y - \alpha x)/\alpha. \tag{3.52}$$

With the new X_r the wedge flow is identical to flow past a flat plate in the first approximation when $X \ll X_r$. That is, the wedge thickness is small in comparison with the thickness of the disturbed-flow region when $X \ll X_r$. Since the merged-layer regime again is present for $X = O(M_\infty^{2\omega} \nu_\infty/u_\infty)$, i.e. for $x = O(\alpha^4)$, the strong-interaction description given above now applies to the region $\alpha^4 \ll x \ll 1$, a region that is shorter than for a flat plate in view of the revised definition for X_r.

In the weak-interaction region for $x \gg 1$, the flow between the shear layer and the strong shock wave from the wedge vertex is, however, described in a different way, in terms of small perturbations about the uniform flow behind the shock wave. A linearized flow description is again appropriate, but both families of waves are present because outgoing waves are reflected from the shock wave; the reflected waves are weak in a numerical sense, but not in an asymptotic sense, since the ratio of reflected-wave strength to incident-wave strength does not vanish under the limit processes considered here. In the blown layer the density is nearly constant, and so the incompressible form of the Bernoulli equation is appropriate in the first approximation.

The required solution in the blown layer was given by Cole & Aroesty (1968). The blowing velocity is taken to be $v_w = \alpha^2 \tilde{v}_{1w} x^{-\frac{1}{2}} = M_\infty^\omega \tilde{v}_{1w} (u_\infty X/\nu_\infty)^{-\frac{1}{2}}$, the same as chosen for the flat plate. For $x \to \infty$, the pressure perturbation is related to u by the Bernoulli equation for incompressible flow and, for matching with the perturbed wedge flow, has the same order of magnitude as the product of $(M_\infty \alpha)^2$ and the ratio of a typical perturbation in streamline slope at the wedge angle. In the blown layer (3.19) and (3.20) are replaced by

$$\rho \sim \tilde{\rho}_{1w} = \text{const.}, \quad u^2 \sim \frac{2}{\gamma M_\infty^2 \tilde{\rho}_{1w}} \{p(x_w) - p(x)\}, \tag{3.53}$$

where again the value of x_w defines a streamline. The solutions for u and p when $x \gg 1$ are expanded in terms of $\tilde{\zeta} = \tilde{\psi}/x^{\frac{1}{2}}$ as

$$u = \alpha x^{-\frac{1}{6}} \tilde{\tilde{u}}_1(\tilde{\zeta}) + \ldots, \quad p = M_\infty^2 \alpha^2 \{\gamma(\gamma+1)/2 + x^{-\frac{1}{3}} \tilde{\tilde{p}}_1 + \ldots\}, \tag{3.54}$$

where $\tilde{\tilde{u}}_1$ is found in terms of $\tilde{\tilde{p}}_1$ from (3.53) and $\tilde{\tilde{p}}_1$ is a constant to be determined later. Again the double tilde is used where necessary to distinguish from quantities defined for $x \ll 1$. The streamline shapes are found, again using $\psi_y = \rho u$ and $\xi = x_w/x$, from

$$\tilde{y} = x^{\frac{2}{3}} \tilde{\tilde{y}}_1(\tilde{\zeta}) + \ldots, \quad \mathrm{d}\tilde{\tilde{y}}_1 = -\left(\frac{\gamma \tilde{\rho}_{1w}}{2\tilde{\tilde{p}}_1}\right)^{\frac{1}{2}} \tilde{v}_{1w} \xi^{-\frac{1}{3}} (1 - \xi^{\frac{1}{3}})^{-\frac{1}{2}} \mathrm{d}\xi. \tag{3.55}$$

The blown layer has the shape of an effective body

$$\tilde{y} \sim \tilde{\tilde{A}}_1 x^{\frac{2}{3}}, \quad \tilde{\tilde{A}}_1 = 4\{\gamma \tilde{\rho}_{1w} \tilde{v}_{1w}^2/(2\tilde{\tilde{p}}_1)\}^{\frac{1}{3}}, \tag{3.56}$$

where $\tilde{\tilde{A}}_1$ is found by integration of (3.55).

In the region between the shear layer and the shock wave the flow is nearly uniform with the flow variables equal to the values obtained from the shock-wave relations. As $x \to \infty$,

$$v = \alpha\{1 + v_1(x, \hat{y}) + \ldots\}, \tag{3.57}$$

$$p = M_\infty^2 \alpha^2 \{\tfrac{1}{2}\gamma(\gamma+1) + p_1(x, \hat{y}) + \ldots\}, \tag{3.58}$$

$$\rho = (\gamma+1)/(\gamma-1) + \rho_1(x, \hat{y}) + \ldots, \tag{3.59}$$

where $|v_1| \ll 1$, $|p_1| \ll 1$, and $|\rho_1| \ll 1$. The perturbations in v, p, and ρ are described by the linearized form of the hypersonic small-disturbance equations (3.1)–(3.3):

$$\rho_{1x}+\frac{\gamma+1}{\gamma-1}v_{1\hat{y}}=0, \quad \frac{\gamma+1}{\gamma-1}v_{1x}+\frac{1}{\gamma}p_{1\hat{y}}=0, \quad p_{1x}-\tfrac{1}{2}\gamma^2(\gamma-1)\rho_{1x}=0, \tag{3.60}$$

where ρ_1 is easily eliminated. Linearized boundary conditions are given at the wedge surface $\hat{y}=0$ and at the undisturbed shock-wave position $\hat{y}=\frac{1}{2}(\gamma-1)x$:

$$v_1(x,0)=\mathrm{d}\tilde{\tilde{A}}(x)/\mathrm{d}x, \quad p_1\left(x,\frac{\gamma-1}{2}x\right)=\gamma(\gamma+1)v_1\left(x,\frac{\gamma-1}{2}x\right), \tag{3.61}$$

where $\tilde{\tilde{A}}(x)=\tilde{\tilde{A}}_1 x^{\frac{2}{3}}$.

The differential equations (3.60) and boundary conditions (3.61) are satisfied by solutions in the self-similar form $x^{-\frac{1}{3}}\mathrm{fn}(\hat{y}/x)$. Since p_1 and v_1 must each satisfy a wave equation, the solutions are known, moreover, to be functions only of $x\pm M_0\hat{y}$, where $M_0=\{\frac{1}{2}\gamma(\gamma-1)\}^{-\frac{1}{2}}$. It follows that

$$\frac{1}{\gamma}p_1=c_1\{x+M_0\hat{y}\}^{-\frac{1}{3}}+c_2\{x-M_0\hat{y}\}^{-\frac{1}{3}}, \tag{3.62}$$

$$-\frac{\gamma+1}{(\gamma-1)M_0}v_1=c_1\{x+M_0\hat{y}\}^{-\frac{1}{3}}-c_2\{x-M_0\hat{y}\}^{-\frac{1}{3}}. \tag{3.63}$$

The integration constants c_1 and c_2 are found from the boundary conditions to be

$$c_2=\frac{k^{\frac{1}{3}}}{\lambda}c_1=\frac{2(\gamma+1)\tilde{\tilde{A}}_1 k^{\frac{1}{3}}}{3(\gamma-1)M_0(k^{\frac{1}{3}}-\lambda)}, \tag{3.64}$$

where

$$k=\frac{2-(\gamma-1)M_0}{2+(\gamma-1)M_0}, \quad \lambda=\frac{(\gamma-1)M_0-1}{(\gamma-1)M_0+1}, \quad M_0=\left(\frac{2}{\gamma(\gamma-1)}\right)^{\frac{1}{2}}. \tag{3.65}$$

The solution to (3.60) and (3.61) for arbitrary $\tilde{\tilde{A}}(x)$ has been discussed by Chernyi (1961). The result is found as an infinite series, since a disturbance reaching the surface contains the effects of infinitely many wave reflections. Chernyi (1961) and Cole & Aroesty (1968) also specialized this solution for a power-law form of $\tilde{\tilde{A}}(x)$; equations (3.62)–(3.65) duplicate their results.

Setting $\hat{y}=0$ in (3.62) gives $\tilde{\tilde{p}}_1$ in terms of $\tilde{\tilde{A}}_1$:

$$\tilde{\tilde{p}}_1=x^{\frac{1}{3}}p_1(x,0)=\frac{2\gamma(\gamma+1)\tilde{\tilde{A}}_1(\lambda+k^{\frac{1}{3}})}{3(\gamma-1)M_0(k^{\frac{1}{3}}-\lambda)}. \tag{3.66}$$

A second relation between $\tilde{\tilde{p}}_1$ and $\tilde{\tilde{A}}_1$ is found from the blown-layer solution (3.56). Eliminating A_1,

$$\tilde{\tilde{p}}_1=2(\gamma\tilde{\rho}_{1\mathrm{w}}\tilde{v}_{1\mathrm{w}}^2)^{\frac{1}{3}}\left(\frac{2\gamma(\gamma+1)(\lambda+k^{\frac{1}{3}})}{3(\gamma-1)M_0(k^{\frac{1}{3}}-\lambda)}\right)^{\frac{2}{3}}. \tag{3.67}$$

For $\gamma=1.4$, $\tilde{\tilde{p}}_1=3.615\,(\tilde{\rho}_{1\mathrm{w}}\tilde{v}_{1\mathrm{w}}^2)^{\frac{1}{3}}$.

4. Numerical results

The strong-interaction solutions are obtained in the limit as $x\to 0$ and $M_\infty x^{\frac{1}{4}}\to\infty$, with $M_\infty y/x^{\frac{3}{4}}$ held fixed. In this limit the non-dimensional velocity u is zero in the

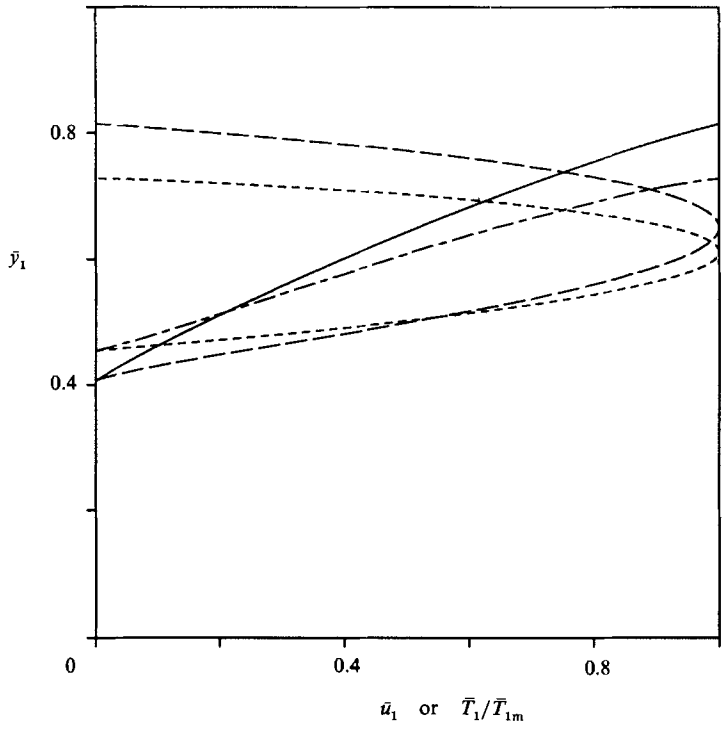

FIGURE 4. Scaled shear-layer solutions in strong-interaction limit, as functions of $M_\infty y/x^{\frac{3}{4}} \sim \bar{y}_1$, for $\tilde{\rho}_{1w}\tilde{v}_{1w}^2 = 0.01$: ——, velocity $\bar{u}_1$ for $\omega = 0.75$; — — —, velocity $\bar{u}_1$ for $\omega = 1.0$; – – –, temperature $\bar{T}_1/\bar{T}_{1m}$ for $\omega = 0.75$; ----, temperature $\bar{T}_1/\bar{T}_{1m}$ for $\omega = 1.0$.

blown layer, increases from zero to one across the viscous layer, and is equal to one in the shock layer. The scaled temperature $M_\infty^2 T$ is zero, in the limit, in the blown layer and in the shock layer, and is $O(1)$ in the viscous layer. For finite but large $M_\infty x^{\frac{1}{4}}$, the first corrections to the zero values of u and $M_\infty^2 T$ in the blown layer are proportional to powers of $(M_\infty x^{\frac{1}{4}})^{-1}$. The remaining parameters are the ratio of specific heats γ, here taken equal to 1.4; the exponent ω in the viscosity law $\mu = T^\omega$; and a blowing parameter $\tilde{\rho}_{1w}\tilde{v}_{1w}^2$, related to the momentum flux normal to the surface.

In the first approximation for the strong-interaction region, the pressures (3.24) and (3.38) in the blown layer and viscous layer are functions of x only and are equal to the pressure (3.10) evaluated at the inner edge of the shock layer. The result (3.44) is $\tilde{p}_1 = \bar{p}_1 = \hat{p}_1(0)$. The quantities $\hat{p}_1(0)/\Delta_1^2$, $\tilde{p}_1^{\frac{1}{2}}\tilde{\Delta}_1$, and $\bar{p}_1^{\frac{1}{2}}\bar{\Delta}_1$ are given by (3.14), (3.27), and (3.43) respectively. With $\Delta_1 = \bar{\Delta}_1 + \tilde{\Delta}_1$ according to (2.21), the pressure p_w at the surface is found for $\gamma = 1.4$ and $\omega = 0.75$ as

$$p_w = \{0.3721 + 3.703(\tilde{\rho}_{1w}\tilde{v}_{1w}^2)^{\frac{1}{2}}\}x^{-\frac{1}{2}} + \ldots. \tag{4.1}$$

If instead $\omega = 1$, the surface pressure becomes

$$p_w = \{0.2221 + 3.703(\tilde{\rho}_{1w}\tilde{v}_{1w}^2)^{\frac{1}{2}}\}x^{-\frac{1}{2}} + \ldots. \tag{4.2}$$

The ratio of the shear-layer thickness $\bar{\Delta}_1$ to the blown-layer thickness $\tilde{\Delta}_1$ is found from (3.27), (3.43), and (3.44), and is seen to decrease as $\tilde{\rho}_{1w}\tilde{v}_{1w}^2$ increases. When $\omega = 0.75$, the ratio is

$$\bar{\Delta}_1/\tilde{\Delta}_1 = 0.119/(\tilde{\rho}_{1w}\tilde{v}_{1w}^2)^{\frac{1}{2}}, \tag{4.3}$$

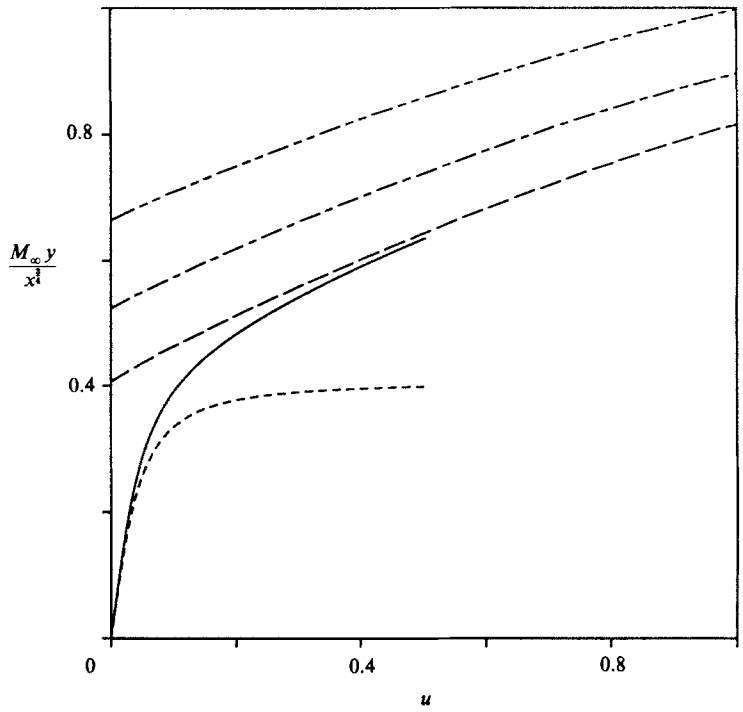

FIGURE 5. Velocity profiles u *vs.* $M_\infty y/x^{\frac{3}{4}}$ in strong-interaction region, for $\omega = 0.75$: ---, shear layer for $\tilde{\rho}_{1w}\tilde{v}_{1w}^2 = 0.01$; - - - -, blown layer for $\tilde{\rho}_{1w}\tilde{v}_{1w}^2 = 0.01$, $M_\infty x^{\frac{1}{4}} = 10$, $\tilde{\rho}_{1w} = 4$; ——, composite for $\tilde{\rho}_{1w}\tilde{v}_{1w}^2 = 0.01$, $M_\infty x^{\frac{1}{4}} = 10$, $\tilde{\rho}_{1w} = 4$; ———, shear layer for $\tilde{\rho}_{1w}\tilde{v}_{1w}^2 = 0.02$; — — — —, shear layer for $\tilde{\rho}_{1w}\tilde{v}_{1w}^2 = 0.04$.

and when $\omega = 1.0$, the constant is replaced by 0.071. Thus the two layer thicknesses are equal when the value of $(\tilde{\rho}_{1w}\tilde{v}_{1w}^2)^{\frac{1}{2}}$ is about 0.1; in the numerical calculations this parameter is taken equal to 0.1 or 0.2. The shock-wave shape for $\omega = 0.75$ is then found from (2.20), (2.21), and (3.14) to be

$$y_s = M_\infty^{-1}\{0.9515 + 9.469(\tilde{\rho}_{1w}\tilde{v}_{1w}^2)^{\frac{1}{2}}\}^{\frac{1}{2}}x^{\frac{3}{4}} + \ldots. \tag{4.4}$$

If $\omega = 1$, the constant 0.9515 is replaced by 0.5680.

The shear-layer velocity and temperature profiles of figure 3 are replotted in figure 4 as functions of $M_\infty y/x^{\frac{3}{4}}$, instead of $\bar{p}_1^{-\frac{1}{2}}M_\infty^3\psi/x^{\frac{1}{4}}$, for two values of the exponent ω and for $\tilde{\rho}_{1w}\tilde{v}_{1w}^2 = 0.01$, i.e. for nearly equal blown-layer and shear-layer thicknesses. The hot low-density shear layer occupies the region $\tilde{\Delta}_1 < M_\infty y/x^{\frac{3}{4}} < \tilde{\Delta}_1 + \bar{\Delta}_1$ and thus has a clearly defined thickness, as shown both by the figure and by the integral of (3.42). The blown layer is defined to be the region $0 < M_\infty y/x^{\frac{3}{4}} < \tilde{\Delta}_1$ between the shear layer and the wall and contains almost all of the blown gas, with the exception of an amount smaller by a factor $O\{(M_\infty x^{\frac{1}{4}})^{-1}\}$ that is entrained in the lower part of the shear layer. The streamline separating free-stream air from the blown gas thus lies within the shear layer. Since the scaled viscosity coefficient in (3.33) and (3.34) is proportional to $\bar{T}^\omega$, and $\bar{T} < 1$, an increase in ω decreases the diffusion rate and therefore decreases the shear-layer thickness $\bar{\Delta}_1$. In figure 4 a change in ω from $\omega = 0.75$ to $\omega = 1.0$ is seen to decrease $\bar{\Delta}_1$ by a factor of about $\frac{2}{3}$, and also, because of coupling through the pressure, to give a small increase in the blown-layer thickness $\tilde{\Delta}_1$, such that sum $\Delta_1 = \bar{\Delta}_1 + \tilde{\Delta}_1$ decreases. Since the shock-wave position $\hat{y}_{1s}$ is proportional to Δ_1, as seen

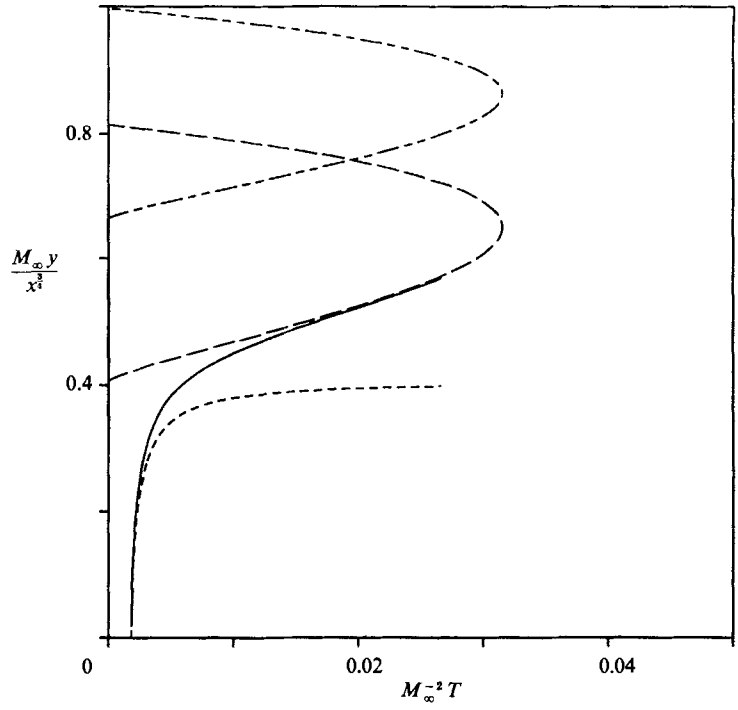

FIGURE 6. Temperature profiles $M_\infty^{-2} T$ *vs.* $M_\infty y/x^{\frac{3}{4}}$ in strong-interaction region, for $\omega = 0.75$: ——, shear layer for $\tilde{\rho}_{1w}\tilde{v}_{1w}^2 = 0.01$; - - - -, blown layer for $\tilde{\rho}_{1w}\tilde{v}_{1w}^2 = 0.01$, $M_\infty x^{\frac{1}{4}} = 10$, $\tilde{\rho}_{1w} = 4$; ——, composite for $\tilde{\rho}_{1w}\tilde{v}_{1w}^2 = 0.01$, $M_\infty x^{\frac{1}{4}} = 10$, $\tilde{\rho}_{1w} = 4$; ————, shear layer for $\tilde{\rho}_{1w}\tilde{v}_{1w}^2 = 0.04$.

in (3.14), the shock-wave slope then decreases, and the pressure also decreases, as shown by (4.1) and (4.2).

In figure 5 the shear-layer velocity u is plotted against $M_\infty y/x^{\frac{3}{4}}$ for $\omega = 0.75$ and for three values of the blowing parameter, $\tilde{\rho}_{1w}\tilde{v}_{1w}^2 = 0.01$, 0.02, and 0.04. Stronger blowing of course moves the shear layer further from the wall and also decreases its thickness slightly. The velocity in the blown layer, smaller by a factor $O\{(M_\infty x^{\frac{1}{4}})^{-1}\}$, is shown for $M_\infty x^{\frac{1}{4}} = 10$, $\tilde{\rho}_{1w}\tilde{v}_{1w}^2 = 0.01$, and $\tilde{v}_{1w} = 0.05$. An inverse composite solution is also shown, obtained by adding the blown-layer and shear-layer solutions for $M_\infty y/x^{\frac{3}{4}}$ in terms of u, for $0 < u < 1$, and subtracting the common part, namely $\bar{A}_1$. This composite is uniformly valid to $O(1)$ in $M_\infty y/x^{\frac{3}{4}}$, since the shear-layer and blown-layer solutions are recovered by taking limits with u fixed and with $M_\infty x^{\frac{1}{4}}u$ fixed, respectively. It would also be possible to obtain a shock-layer solution for $u - 1$ and to use the results of Bush (1966) to show a smooth joining with the shear-layer solution.

Profiles of the scaled temperature $M_\infty^{-2} T$ are shown in figure 6 for two of the cases, $\tilde{\rho}_{1w}\tilde{v}_{1w}^2 = 0.01$ and 0.04, shown in figure 5. The maximum temperature T_m is seen to be about $T_m = 0.0315 M_\infty^2 T_\infty$, for the selected values $\gamma = 1.4$ and $\omega = 0.75$. This value of T_m is less than $\frac{1}{6}$ of the isentropic stagnation temperature T_0, and so real-gas effects are delayed to a somewhat higher Mach number than if the full T_0 were reached. A composite solution for $M_\infty y/x^{\frac{3}{4}}$ in terms of $M_\infty^{-2} T$ is shown for the same numerical values as in figure 5. To allow the correct T at $y = 0$, the curve has been displaced downward by a small (higher-order) amount; the correction is chosen to decrease linearly with T and disappears at $T = T_m/T_\infty$.

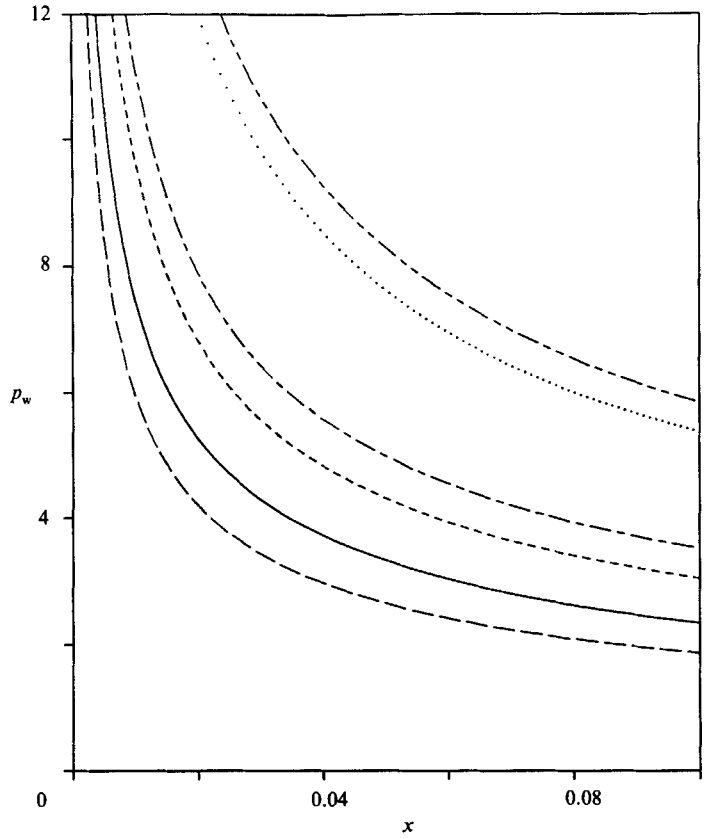

FIGURE 7. Surface pressure distribution p_w *vs.* x, in strong-interaction region: ——, $\tilde{\rho}_{1w}\tilde{v}_{1w}^2 = 0.01$ and $\omega = 0.75$; – – –, $\tilde{\rho}_{1w}\tilde{v}_{1w}^2 = 0.01$ and $\omega = 1.0$; — — —, $\tilde{\rho}_{1w}\tilde{v}_{1w}^2 = 0.04$ and $\omega = 0.75$; - - - -, $\tilde{\rho}_{1w}\tilde{v}_{1w}^2 = 0.04$ and $\omega = 1.0$; ——— —, $\tilde{\rho}_{1w}\tilde{v}_{1w}^2 = 0.16$ and $\omega = 0.75$; ....., $\rho_{1w}\tilde{v}_{1w}^2 = 0.16$ and $\omega = 1.0$.

Figure 7 shows the strong-interaction pressure for three values of the blowing parameter $\tilde{\rho}_{1w}\tilde{v}_{1w}^2$, for $\omega = 0.75$ and for $\omega = 1.0$. As predicted by (4.1) and (4.2), the pressure is linear in $(\tilde{\rho}_{1w}\tilde{v}_{1w}^2)^{\frac{1}{2}}$ and decreases as ω increases.

The weak-interaction pressure, for $X \gg X_r$, differs from a constant value by $O(x^{-\frac{1}{3}})$, as in the solutions (3.28) for a flat plate and (3.62) for a wedge. A calculation for $X = O(X_r)$, however, would require numerical solution of partial differential equations in the shock layer and shear layer. Nevertheless, since the extensions (unwarranted, to be sure) of the asymptotic solutions toward $X = X_r$ do not lie very far apart, a reasonable idea of the approximate surface pressure in this region can be found quite easily by interpolating in some very simple arbitrary way between the strong-interaction and weak-interaction results. The interpolation formula adopted here is

$$p_w - 1 = r\{p_w^{(\text{strong})} - 1\} + (1-r)\{p_w^{(\text{weak})} - 1\} = r\tilde{p}_1 x^{-\frac{1}{2}} + (1-r)\tilde{\tilde{p}}_1 x^{-\frac{1}{3}}, \tag{4.5}$$

where $\tilde{\tilde{p}}_1$ is given by (3.32), and

$$r = \frac{1}{\cosh \beta x}, \quad \beta = \cosh^{-1} 2, \tag{4.6}$$

so that r decreases from 1 to 0 as x increases from 0 to ∞. The free parameter β in the interpolation formula has been chosen so that $r = \frac{1}{2}$ when $x = 1$. That is, at $x =$

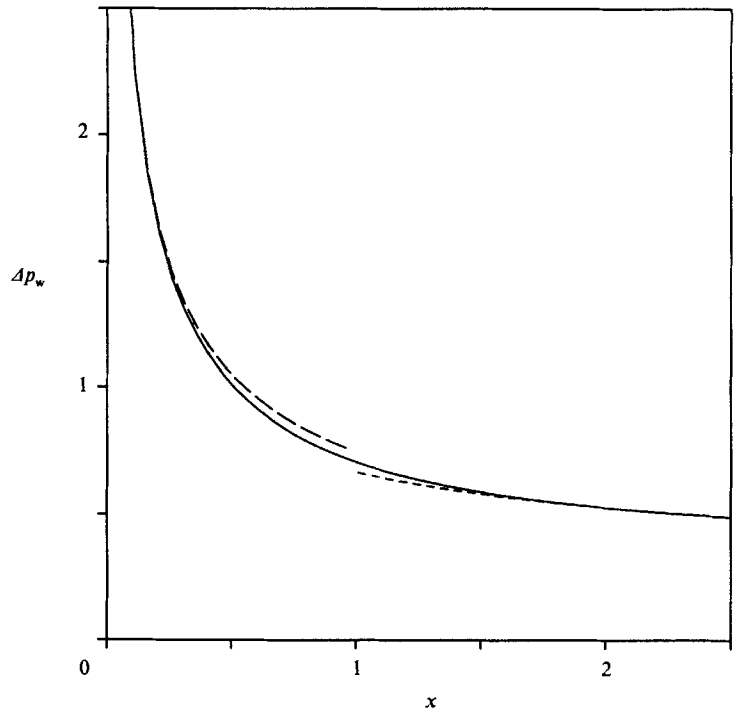

FIGURE 8. Surface pressure $\Delta p_w = \{p_w - \frac{1}{2}\gamma(\gamma+1)(M_\infty\alpha)^2\}/(M_\infty\alpha)^2$ *vs.* $x = X/\{M_\infty^{2\omega}\alpha^{-4}\nu_\infty/u_\infty\}$ for thin wedge, for $\tilde{\rho}_{1w}\tilde{v}_{1w}^2 = 0.01$ and $\omega = 0.75$: – – –, strong-interaction solution; - - - -, weak-interaction solution; ——, interpolated solution.

1 the interpolated solution is chosen to lie halfway between the pressures that would be predicted if the strong-interaction and weak-interaction solutions were evaluated there (beyond their respective regions of validity $x \ll 1$ and $x \gg 1$). For a thin wedge, the required rescaling gives

$$\frac{p_w}{(M_\infty\alpha)^2} - \tfrac{1}{2}\gamma(\gamma+1) = r\tilde{p}_1 x^{-\frac{1}{2}} + (1-r)\tilde{\tilde{p}}_1 x^{-\frac{1}{3}}, \tag{4.7}$$

where now $x = X/\{M_\infty^{2\omega}\alpha^{-4}\nu_\infty/u_\infty\}$ and $\tilde{\tilde{p}}_1$ is given by (3.67). Interpolated surface pressures for a wedge are shown in figure 8. Although the error appears to be small, it should be remembered that the value (4.6) for β is arbitrary, and a change in β would shift the location of the interpolated curve. The function r is likewise arbitrary, and there is no theoretical basis for the suggested choice; the accuracy of the interpolated curve in figure 8 remains uncertain in the absence of a numerical solution for $X = O(X_r)$.

Additional numerical results for a wedge in the case of uniform surface temperature, including the integrated force change as a function of blowing rate and other parameters, have been given by Matarrese, Messiter & Adamson (1990).

5. Concluding remarks

The extension of hypersonic viscous strong-interaction theory to permit large surface blowing velocity requires that choices be made among several possibilities for the surface boundary conditions. Two constraints have been imposed: the perfect-

gas law must be satisfied, and the blown-layer thickness is taken to be of the same order of magnitude as the viscous- and shock-layer thicknesses. Here the density of the blown gas has been chosen to be of the same order as the undisturbed air density and to be constant at the wall; the corresponding form for the blowing velocity is then fixed. Other choices can be made, leading to differences in the blown-layer solution and in some cases differences in the conditions at the lower 'edge' of the shear layer.

Even a first approximation is found to introduce some subtleties. Although the three appropriate limit processes have been successfully applied to give self-consistent asympotic flow representations in the three layers, the matching of solutions in adjacent layers is not complete, and would have to be refined if higher approximations, presumably proceeding in powers of x and $(M_\infty x^{-\frac{1}{4}})^{-1}$, were desired. Moreover, the results do not reduce in a simple way to the solutions for weak blowing. As for incompressible flow, a special limiting case would have to be considered in the neighbourhood of blowoff, when the amount of injected mass is close to the mass entrained in the lower part of the free shear layer. Finally, numerical solution of the shear-layer equations for $\omega \neq 1$ was not successful with a straightforward shooting technique, and ultimately was carried out by an approach to the desired result through neighbouring solutions.

In the present fomulation the scaled results contain only a single blowing parameter which measures the normal momentum flux at the surface. (The ratio of specific heats and the exponent in the viscosity law of course appear as well.) As an obvious extension it is planned to consider the injected gas as different from air, so that in general one more differential equation is required, with one or more additional non-dimensional parameters. Further numerical studies will then be carried out. It is also anticipated that the present formulation will serve as a useful test case for comparison with numerical Euler and Navier–Stokes codes.

This research was supported in part by the US Army Strategic Defense Command.

REFERENCES

Brown, S. N. & Stewartson, K. 1975 A nonuniqueness of the hypersonic boundary layer. *Q. J. Mech. Appl. Maths* **28**, 75–90.

Bush, W. B. 1966 Hypersonic strong-interaction similarity solutions for flow past a flat plate. *J. Fluid Mech.* **25**, 51–64.

Chernyi, G. G. 1961 *Introduction to Hypersonic Flow.* Academic.

Cole, J. D. & Aroesty, J. 1968 The blowhard problem – inviscid flows with surface injection. *Intl J. Heat Mass Transfer* **11**, 1167–1183.

Hayes, W. D. & Probstein, R. F. 1959 *Hypersonic Flow Theory.* Academic.

Kassoy, D. R. 1971 On laminar boundary-layer blowoff. Part 2. *J. Fluid Mech.* **48**, 209–228.

Klemp, J. B. & Acrivos, A. 1972 High Reynolds number flow past a flat plate with strong blowing. *J. Fluid Mech.* **51**, 337–356.

Kubota, T. & Fernandez, F. L. 1968 Boundary-layer flows with large injection and heat transfer. *AIAA J.* **6**, 22–28.

Lee, R. S. & Cheng, H. K. 1969 On the outer-edge problem of a hypersonic boundary layer. *J. Fluid Mech.* **38**, 161–179.

Li, T.-Y. & Gross, J. F. 1961 Hypersonic strong viscous interaction on a flat plate with surface mass transfer. *Proc. 1961 Heat Transfer & Fluid Mech. Inst.*, pp. 146–160.

Matarrese, M. D. & Messiter, A. F. 1990 A numerical method for the self-similar hypersonic viscous shear layer. *J. Comp. Phys.* (submitted).

MATARRESE, M. D., MESSITER, A. F. & ADAMSON, T. C., JR. 1990 Control of hypersonic aerodynamic forces with surface blowing. *AIAA Paper* 90-0602.

SMITH, F. T. & STEWARTSON, K. 1973*a* On slot injection into a supersonic laminar boundary layer. *Proc. R. Soc. Lond.* A **332**, 1–22.

SMITH, F. T. & STEWARTSON, K. 1973*b* Plate-injection into a separated supersonic boundary layer. *J. Fluid Mech.* **58**, 143–159.

STEWARTSON, K. 1964 *The Theory of Laminar Boundary Layers in Compressible Fluids.* Oxford University Press.

VAN DYKE, M. D. 1954 A study of hypersonic small-disturbance theory. *NACA Rep.* 1194 (supersedes *TN* 3173, 1954).

WALLACE, J. & KEMP, N. 1969 Similarity solutions to the massive blowing problem. *AIAA J.* **7**, 1517–1523.